1

# Comparison of ammonia air concentration before and during the spread of COVID-19 in Lombardy (Italy) using ground-based and satellite data

5

6

Daniela Lovarelli[1], Davide Fugazza*[1], Michele Costantini[1], Cecilia Conti[1], Guglielmina Diolaiuti[1], Marcella Guarino[1]

[1] Department of Environmental Science and Policy, Università degli Studi di Milano, via G. Celoria, 2, 20133 Milano, Italy

*Corresponding author: davide.fugazza@unimi.it; +39 0250315566

14

15

18

**Abstract**

Several anthropogenic activities have undergone major changes following the spread of the COVID-19 pandemic, which in turn has had consequences on the environment. The effect on air pollution has been studied in detail in the literature, although some pollutants, such as

23   ammonia (NH$_3$), have received comparatively less attention to date. Focusing on the case of

24   Lombardy in Northern Italy, this study aimed to evaluate changes in NH$_3$ atmospheric

25   concentration on a temporal scale (the years from 2013 to 2019 compared to 2020) and on a

26   spatial scale (countryside, city, and mountain areas). For this purpose, ground-based (from

27   public air quality control units scattered throughout the region) and satellite observations

28   (from IASI sensors on board MetOp-A and MetOp-B) were collected and analyzed. For ground-

29   based measurements, a marked spatial variability is observed between the different areas

30   while, as regards the comparison between periods, statistically significant differences were

31   observed only for the countryside areas (+31% in 2020 compared to previous years). The

32   satellite data show similar patterns but do not present statistically significant differences

33   neither between different areas, nor between the two periods. In general, there have been no

34   reduction effects of atmospheric NH$_3$ as a consequence of COVID-19. This calls into question

35   the role of the agricultural sector, which is known to be the largest responsible for NH$_3$

36   emissions. Even if the direct comparison between the two datasets shows little correlation,

37   their contextual consideration allows making more robust considerations regarding air

38   pollutants.

39

## 1. Introduction

41   Ammonia (NH$_3$) is an air pollutant of increasing environmental concern, whose emissions are

42   primarily anthropogenic, released mainly from the agricultural sector by field application of

43   synthetic fertilizers and manure management (Van Damme et al., 2015). NH$_3$ causes a series

44   of cascading negative effects that damage both ecosystem biodiversity due to acidification and

45   nitrogen enrichment (EMEP Centre on Emission Inventories and Projections, 2020; Erisman et

46  al., 2007; European Commission, 2005) and human health (Van Damme et al., 2014), being a

47  precursor of secondary fine particulate matter ($PM_{2.5}$) (Lovarelli et al., 2020; Perone, 2021).

48  The damages to public health and ecosystems have been evaluated in 10-25 €/kg $NH_3$

49  (Executive Body of the Convention on Long-Range Transboundary Air Pollution, 2019). For

50  these reasons, in recent decades, international integrated policies have been increasingly

51  interested in quantifying, monitoring, and limiting $NH_3$ emissions. Despite the reduction

52  obtained in absolute terms since 1990, in 2018, agriculture accounted for 93% of $NH_3$

53  emissions in relative terms in the European Union, still showing the criticality of this sector

54  (EEA, 2019).

55  The reduction of $NH_3$ emissions is a complex process. First of all, measuring this compound is

56  not easy, which also makes accurate monitoring difficult. The most widely used methodologies

57  to date are measurements through ground-based instruments and satellite-based remote-

58  sensing (Nair & Yu, 2020). However, each of these two techniques has advantages and

59  problems. The ground-based measurements currently allow understanding the evolution of

60  the atmospheric concentrations over time at ground level, but they are affected by local spatial

61  and meteorological variability. Indeed, $NH_3$ volatilization from main primary sources (fertilizers

62  and manure) is influenced by weather parameters such as wind speed, rainfall, and

63  temperature, among others (Brentrup et al., 2000). Given the high variability related to $NH_3$

64  emissions, a geographically dense network of control units can be a useful method to fulfill

65  monitoring requirements. However, due to the stickiness of $NH_3$ to observational instruments,

66  the control units that collect $NH_3$ data are normally fewer per unit area than those used to

67  measure other air pollutants (Van Damme et al., 2015). Satellite remote sensing, on the other

68  hand, is based on the distinction of the $NH_3$ spectrum in the gas-phase by means of infrared

69  spectrometers and allows to obtain a broad spatial coverage (both superficial and vertical) of

70    $NH_3$ atmospheric concentrations, but the measurements available to date suffer from

71    temporal discontinuity because deployed instrumentation is not onboard geostationary

72    satellites (Nair & Yu, 2020). Furthermore, the reliability of the measurements at night or in the

73    presence of clouds decreases. Ultimately, since the two methods compensate, at least

74    partially, the respective limitations, considerations on atmospheric $NH_3$ pollution made by

75    integrating both types of measurement can be more solid and comprehensive.

76    During the worldwide spread of Coronavirus Disease 2019 (COVID-19) in 2020, attention on air

77    quality and the need to understand changes in the presence of pollutants in the atmosphere

78    increased considerably. In literature, several studies have focused on the relationships among

79    the COVID-19 outbreak, government actions to contain the spread of the infection and air

80    pollution (Nuñez-Delgado et al., 2021; Zambrano-Monserrate et al., 2020). Among the

81    European countries, Italy was the first in which the infection was detected in 2020, and which

82    suffered a rapid spread of the infection in the first months of the year; this led the government

83    to implement partial restrictions (e.g., establishment of a "red zone" in some municipalities in

84    Northern Italy on 23 February, and subsequent interruption of school and university teaching

85    in attendance). Then, heavy restrictions were introduced starting on 8 March, until on 23

86    March a nationwide lockdown was declared. Only industries deemed essential, such as food

87    and pharmaceutical supply chains, and the agrifood sector were allowed to remain

88    operational. This lasted officially until 3 May (DPCM, 2020).

89    As concerns the Po Valley in Northern Italy, where air pollution is recognized as being normally

90    high (Raffaelli et al., 2020), the lockdown period has led to significant reductions in

91    atmospheric concentrations of pollutants such as $PM_{2.5}$, $PM_{10}$, nitrogen oxides ($NO_x$) and

92    others (e.g., carbon monoxide and benzene) (Buganza et al., 2020; Collivignarelli et al., 2020;

93    Deserti et al., 2020). On the other hand, the effect of the pandemic on $NH_3$ concentration has

94  received comparatively less attention (Gualtieri et al., 2020; Lovarelli et al., 2020), although

95  Northern Italy, and in particular Lombardy, is one of the leading regions for agriculture. Here,

96  livestock production accounts for around 52% of pigs (ISMEA, 2019a), 20% of meat and dairy

97  cattle (ISMEA, 2019b, c), and 17% of poultry (ISMEA, 2020) of the whole Country. The lower

98  interest towards $NH_3$, compared to PM concentrations could be explained by the identification

99  of PM particles as possible vectors for transporting the SARS-CoV-2 virus and for their

100  responsibility for respiratory and cardiovascular diseases (Li et al., 2018; Srivastava, 2021).

101  However, $NH_3$ influence on secondary aerosol is significant as it is a recognized precursor

102  (Perone, 2021). Moreover, Zheng et al. (2020) and Manigrasso et al. (2020) discussed the

103  possibility that SARS-CoV-2 spread is favored by a mild alkaline pH of airborne particles, and

104  thus related to ammonia-polluted environments such as the Po Valley. To support this

105  hypothesis, in the world 28 hotspots were identified with an $NH_3$ column concentration above

106  0.5 mg/m$^2$, which were linked to either biomass burning and fires or (and especially)

107  agricultural areas, in particular with agricultural valleys surrounded by mountains, such as the

108  case of Po valley in Northern Italy. Perone (2021) also identified cities in Northern Italy as those

109  with the highest mortality risk in the country.

110  The aim of this study is to analyze $NH_3$ air concentration in Lombardy, the region most affected

111  by the pandemic (Altuwayjiri et al., 2021; Bonati et al., 2021; Perone, 2021), by using both data

112  from control units at ground level and satellite observations to evaluate the temporal and

113  spatial scale of $NH_3$ concentration before and during lockdown (i.e., the strict national

114  lockdown occurred in Spring 2020), highlighting relationships, similarities or differences

115  between these two measurement solutions.

116

## 2. Methods

### 2.1. Data collection of ground-based observations

Ground-based observations were retrieved from the database of the Regional Environmental Protection Agency of Lombardy (ARPA Lombardia, 2020). Data from all the control units collecting $NH_3$ measurements in the Lombardy Region were considered; overall data from 12 control units were available. These latter measure $NH_3$ indirectly through special analyzers using the chemiluminescence technique, by which $NH_3$ is first oxidized to nitrogen oxide (NO) and its concentration in the air sample is measured alongside NO and $NO_2$ (nitrogen dioxide). In particular, hourly data on air $NH_3$ concentration (expressed as $\mu g/m^3$) collected by the control units in question were sourced.

Furthermore, from the same ARPA Lombardia control units and for the same period, the daily weather parameters of temperature (T; °C), relative humidity (RH; %), rainfall (R; mm) and wind speed (W; m/s) were downloaded to consider their effects on $NH_3$ air concentration. The main characteristics of the control units used to retrieve these data are shown in **Table 1**.

| Province | Station Name | Analyzer model | Longitude (E°) | Latitude (N°) | Altitude (m) | Zoned as |
|---|---|---|---|---|---|---|
| Cremona | Corte de Cortesi | API 201E | 10.0062 | 45.2785 | 57 | Country |
| Cremona | Fatebenefratelli | TEI 17i | 10.0438 | 45.1425 | 43 | City |
| Cremona | Gerre Borghi | TEI 17i | 10.0692 | 45.1095 | 36 | City |
| Lecco | Colico | TEI 17i | 9.3847 | 46.1381 | 229 | Mountain |
| Lecco | Moggio | TEI 17i | 9.4975 | 45.9128 | 1194 | Mountain |
| Lodi | Bertonico | API 201E | 9.6663 | 45.2335 | 65 | Country |
| Mantua | Schivenoglia | TEI 17i | 11.0761 | 45.0169 | 12 | Country |

| Milan | Pascal | API 201E | 9.2355 | 45.4790 | 122 | City |
|-------|--------|----------|--------|---------|-----|------|
| Pavia | Folperti | TEI 17i | 9.1646 | 45.1947 | 77 | City |
| Pavia | Sannazzaro | ENVEA AC32e | 8.9042 | 45.1028 | 87 | Country |

133 **Table 1.** List of the control units used. Their location is provided as well as the grouping in

134 different zones.

135

136 All control units were distinguished in "city", "country" (short for countryside) or "mountain"

137 stations, to investigate the effect of COVID-19 on $NH_3$ air concentration in the city, most

138 densely populated and characterized by traffic jams and industrial activities, in the countryside,

139 where agricultural and livestock activities are most concentrated, and in mountain areas. This

140 grouping was based on the zoning of Lombardy for air quality monitoring according to the

141 Italian legislative decree 155/10 under the directive 50/08/CE on ambient air quality and

142 cleaner air for Europe (ARPA Lombardia, 2020). According to the previous regulations, the

143 stations located in *urban agglomerations* or *highly urbanized plains* have been considered as

144 "city" stations, those located in the *plain area* as "country" and finally those located in the *pre-*

145 *Alps, Apennines and mountains* as "mountain". The same grouping of stations was also adopted

146 by Lonati and Cernuschi (2020). The zone shapefile was obtained from the Lombardy region

147 geo-portal website (http://www.geoportale.regione.lombardia.it/) with the zone classification

148 carried out at the municipality level. **Figure 1** shows the regional zoning for Lombardy and the

149 geographical position of each control unit. To further investigate the land cover in each zone,

150 the Corine Land Cover (CLC) classification (Feranec, 2016) from 2018 was reclassified to a

151 binary layer with the classes agriculture/other. Agricultural land cover was 87% in the country

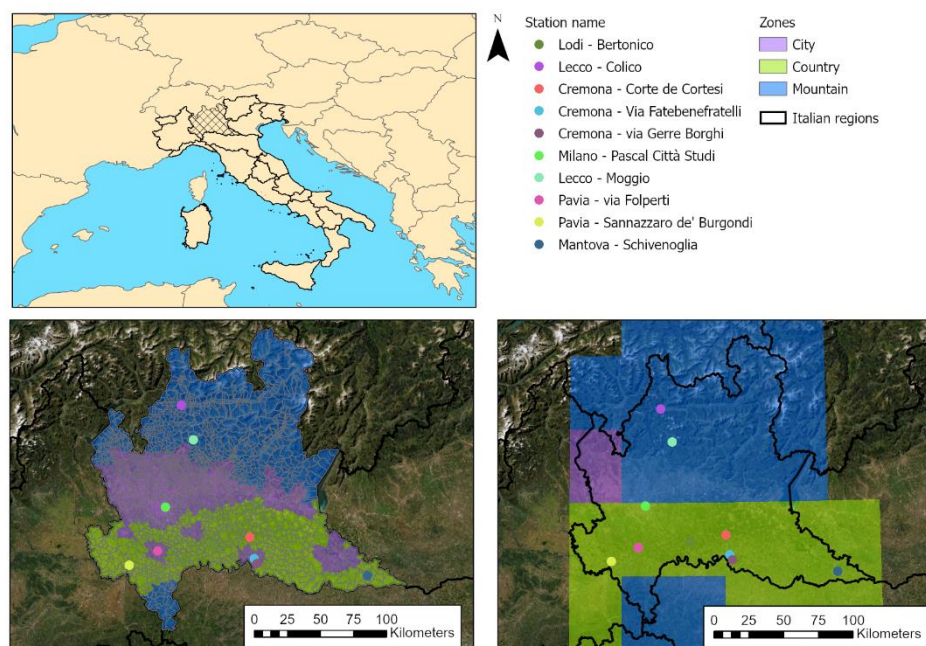152 class, 55% in the city class and 14% in the mountain class.

153

154

155    **Figure 1.** Zoning of the Lombardy region (Northern Italy) in city (violet colored), country (green

156    colored), and mountain (blue colored) zones. Colored dots represent the position of every

157    ground-based control unit. Bottom-left: original zoning; bottom-right: the zoning resampled to

158    IASI pixels

159

160    The temporal coverage of the collected data goes from the beginning of 2013 to the end of

161    October 2020. This period was selected because the same data were available also from the

162    satellite dataset. Some data were lacking or were characterized by excessive uncertainty;

163    therefore, the dataset was cleaned before data processing. With respect to ground-based

164    control units, $NH_3$ concentrations not included in ±3 standard deviations were excluded from

165    the dataset. Data were averaged as daily measures in order to be merged with the weather

166    data for further analyses. All data were grouped in 2 periods to allow comparisons between

167    normal living conditions and the period of the pandemic: the first included data from 2013 to

168    2019, while the second those of 2020.

169 Statistical analyses were conducted using SAS version 9.4 (SAS Institute, Cary, NC, USA)

170 statistical software. Descriptive and multivariate statistics were carried out on each

171 meteorological variable and on $NH_3$ concentration. A general Linear Model procedure (GLM

172 Proc) was carried out to identify a model predicting the air concentration of $NH_3$ based on the

173 unit zoning, local weather, monitoring period, and their interactions. In particular, in the model

174 the following class parameters were included: (i) the period, with the 2 levels of 2013-2019

175 and 2020, and (ii) the zone, with the 3 levels of city, country, and mountain; the weather

176 variables of temperature, rainfall and wind speed and the months of the year were included as

177 well, together with their interactions for (i) year, zone and month, and (ii) temperature, rainfall

178 and wind speed.

179

180 **2.2 Data collection of remote sensing observations**

181 Remote sensing data were retrieved from the online freely available database of the IASI

182 sensor (https://iasi.aeris-data.fr/nh3/), which is the Infrared Atmospheric Sounding

183 Interferometer onboard the ESA's (European Space Agency) MetOp satellites. In particular,

184 data observed by the MetOp-A and MetOp-B satellites were obtained for the period 2013-

185 2020, as MetOp-B became operational in early 2013, and thus data from two satellites were

186 available to obtain a higher number of observations. While a third satellite, MetOp-C has also

187 been operational since 2019, IASI data from this platform were not used to avoid introducing

188 a bias in the later period of the dataset. For both satellites, daily level 2 products were

189 downloaded, which report total column $NH_3$ in molecules/cm$^2$ and their relative uncertainty

190 (in percentage) for discrete points observed by the satellite with an approximate footprint of

191 12 km (at nadir). Only daytime observations were used, as these are considered more accurate

192 owing to the larger thermal contrast compared to nighttime observations (Van Damme et al.

193     2014). As cloud cover and thermal contrast in the atmospheric column greatly reduce the

194     number of available measurements, daily observations lying partially or entirely within the

195     Lombardy region were spatially re-gridded to a 0.5°x0.5° grid (for a total of 26 grid points) and

196     temporally averaged to obtain monthly means. This grid size is similar to the choice adopted

197     by Van Damme et al. (2014) and allowed us to obtain on average 100 measurements per grid

198     cell per month, thus producing more statistically robust $NH_3$ monthly estimations. The

199     averaging was weighted based on the uncertainty of each measurement, following the

200     procedure described by Van Damme et al. (2014), i.e. (equation 1).

201     $\bar{x} = \frac{\sum w_i x_i}{\sum w_i}$     (1)

202     Where $w_i$ is the reciprocal of uncertainty of the measurement, i.e. $1/\sigma^2$ and σ is the error of the

203     total column retrieval on a pixel basis.

204     The uncertainty of each monthly average was then expressed as

205     $\bar{\sigma} = \frac{\sum \frac{1}{\sigma_i}}{\sum \frac{1}{\sigma_i^2}}$     (2)

206     Moreover, it was established to discard monthly means for which the uncertainty was higher

207     than 75% and measurements were fewer than 10 (30% of a month), as per recommendations

208     by Van Damme et al. (2014).

209     Similar to the methodology adopted for the ground-based control units, satellite-based

210     measurements were also divided into two periods, i.e., 2013-2019 and 2020, and classified as

211     "city", "country" or "mountain" based on the areas defined by ARPA Lombardia. In this case,

212     the analysis was limited to the months from January to June owing to the unavailability of IASI

213     data from June 2020 onwards at the time of writing. The zone shapefile was transformed to a

214     raster and resampled to the same 0.5x0.5° grid used for IASI observations; each IASI pixel was

215     then classified by assigning to it the zone with the largest count within the pixel (see Fig.1). In

216    addition, the CLC 2018 was resampled to the IASI grid and the percentage of agricultural land

217    use was counted for each pixel. In the country zone, agricultural land use ranged between 50%

218    and 83% except for one pixel (21%). In the mountain zone, it ranged between 4% and 21%

219    while in the city zone it was 13%.

220    Statistical analyses were also conducted using SAS version 9.4 (SAS Institute, Cary, NC, USA)

221    statistical software, with a General Linear Model procedure (GLM Proc) similar to the ground-

222    based dataset; also in this case, a model predicting $NH_3$ air concentration based on the units

223    zoning, local weather, monitoring period and their interactions was carried out for satellite

224    data. The statistical model used for satellite data was the same as for ground-based data, to

225    allow the best comparability of results; therefore, the parameters included in the model were

226    class parameters for the period (levels of 2013-2019 and 2020) and for the zone (3 levels of

227    city, country, and mountain) and the weather variables of temperature, rainfall and wind

228    speed, the months of the year and the interactions among year, zone and month, as well as

229    temperature, rainfall and wind speed.

230    To complement satellite observations with meteorological data in a similar way as done for

231    ground $NH_3$ measurements, daily temperature, rainfall and wind speed from the reanalysis

232    model ERA5 (European center for meteorology and weather forecast reanalysis) at 0.25°x0.25°

233    resolution were obtained. The values were then regridded to the same 0.5°x0.5° grid of IASI

234    observations and averaged to monthly values to conduct the GLM procedure. The steps of the

235    adopted methodology are summarized for both ground-based and remote sensing
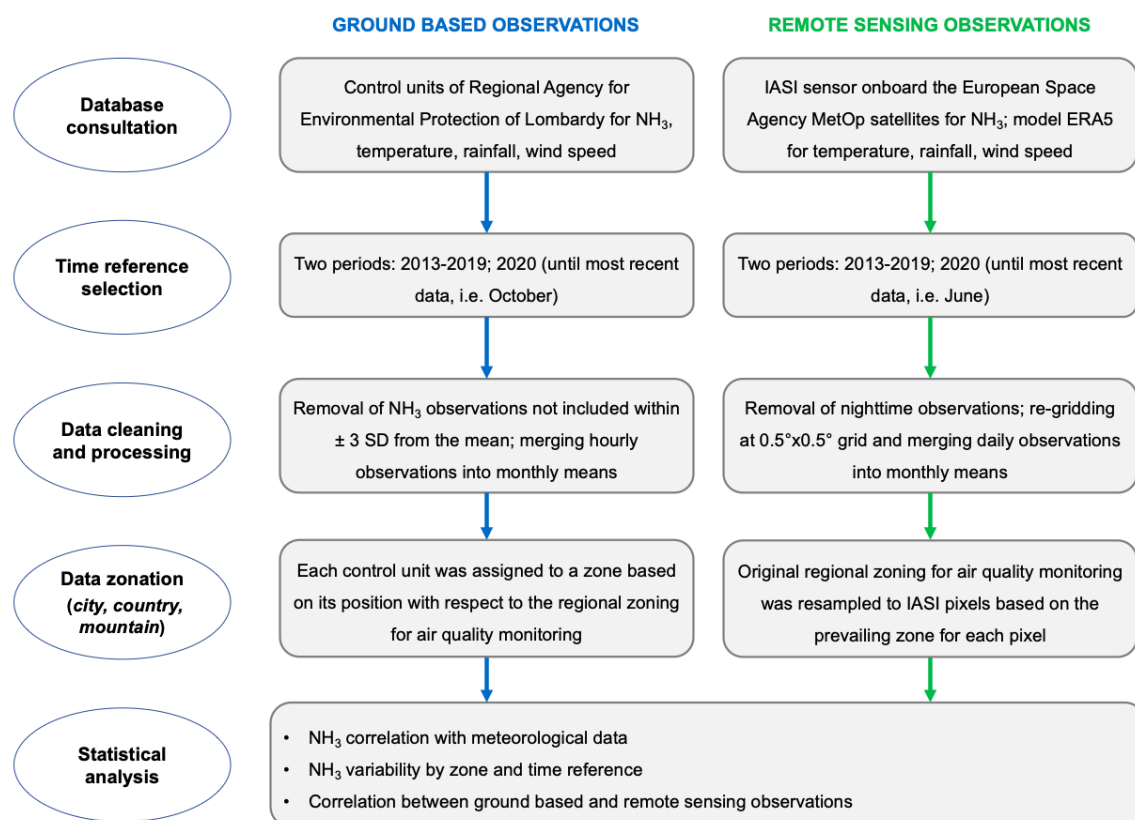
236    observations in **Figure 2**.

**GROUND BASED OBSERVATIONS**

**REMOTE SENSING OBSERVATIONS**

Database consultation
- Control units of Regional Agency for Environmental Protection of Lombardy for $NH_3$, temperature, rainfall, wind speed
- IASI sensor onboard the European Space Agency MetOp satellites for $NH_3$; model ERA5 for temperature, rainfall, wind speed

Time reference selection
- Two periods: 2013-2019; 2020 (until most recent data, i.e. October)
- Two periods: 2013-2019; 2020 (until most recent data, i.e. June)

Data cleaning and processing
- Removal of $NH_3$ observations not included within ± 3 SD from the mean; merging hourly observations into monthly means
- Removal of nighttime observations; re-gridding at 0.5°x0.5° grid and merging daily observations into monthly means

Data zonation (*city, country, mountain*)
- Each control unit was assigned to a zone based on its position with respect to the regional zoning for air quality monitoring
- Original regional zoning for air quality monitoring was resampled to IASI pixels based on the prevailing zone for each pixel

Statistical analysis
- $NH_3$ correlation with meteorological data
- $NH_3$ variability by zone and time reference
- Correlation between ground based and remote sensing observations

237

238    **Figure 2.** Flow chart summarizing the main phases of the methodology adopted to organize

239    and analyze the dataset.

240

241    **3. Results**

242    **3.1 Ground-based measurement**

243    For what concerns $NH_3$ air concentrations, **Figure 3** reports the average concentration

244    ($\mu g/m^3$) for the control units according to the classification in the zones of city, country, and

245    mountain, with the mean and standard error for each month of the two periods 2013–2019

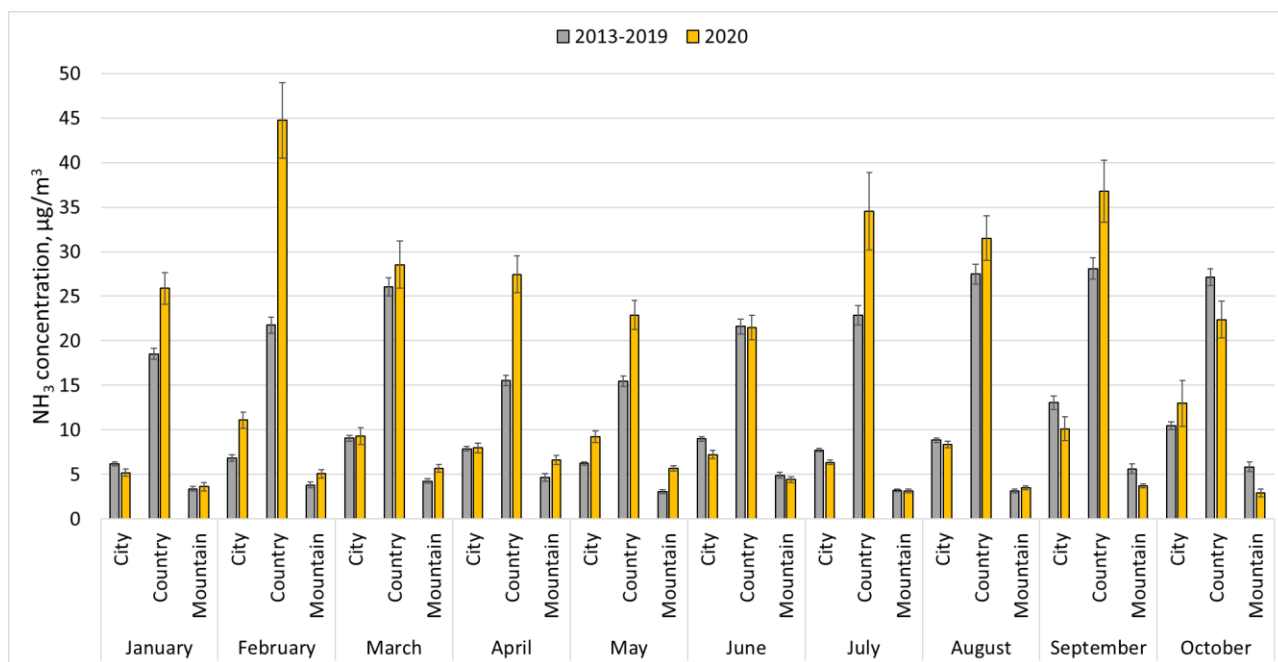246    and 2020.

247

248



Figure 3. Mean and standard error of NH$_3$ concentration, expressed in µg/m$^3$, per zone, month and period.

In both periods, the highest NH$_3$ concentrations can be observed for countryside stations. These stations are located in areas near agricultural production sites, whose seasonal practices affect mostly NH$_3$ emissions. Statistically significant differences can be found among the three zones, with country zones showing much higher concentrations than stations located in city and mountain zones. In particular, the mean yearly value for country zones was 22.5 and 29.5 µg/m$^3$ for 2013-2019 and 2020, respectively. The highest concentrations were recorded in August and September for 2013-2019 (27.5 and 28.1 µg/m$^3$, respectively) and in February and September for 2020 (44.7 and 36.8 µg/m$^3$, respectively). The lowest average value of NH$_3$ concentration in the country zone (21.5 µg/m$^3$, June 2020) was higher than the highest of city and mountain zones (13.0 and 6.6 µg/m$^3$, October and April 2020, respectively).

In all cases, mountain stations show the lowest concentrations, with 2020 higher than 2013-2019 in all months except for June, July, September, and October. The yearly average is equal

264  to 4.2 and 4.4 µg/m$^3$ in 2013-2019 and 2020, respectively. The city zone has intermediate

265  values, with a yearly average equal to 8.6 and 8.8 µg/m$^3$ for 2013-2019 and 2020, respectively.

266  Although for half the months considered, the city zone $NH_3$ concentration was higher in 2020

267  than in the previous period (i.e., February, March, April, May, and October), the annual average

268  is still slightly higher in 2020. Interestingly, the months in which $NH_3$ in the city was higher than

269  in the previous periods were the same months in which the strictest lockdown was in progress

270  (i.e., spring 2020). A similar observation can be done with respect to the mountain zone.

271  Both country and city zones showed higher $NH_3$ concentration in 2020 than in the previous

272  period in February, March, April, and May. Such higher concentration, especially the peak

273  observed in February, can be attributed to manure management and manure field spreading.

274  In particular, because field application of manure can be carried out depending on the

275  constraints fixed by crops cultivation (sowing periods), by laws (European nitrates directive

276  91/676/EEC and the regional action programs for the protection of water pollution), as well as

277  by weather conditions (field spreading can be carried out when field conditions permit it, such

278  as when no rainfall occurs), quite strict temporal windows can be identified during the year.

279  Therefore, slurry application, and the related $NH_3$ air concentration were higher at the

280  beginning of 2020 than in previous years probably because the unfavorable weather conditions

281  of the previous autumn (i.e., in October 2019 high rainfall was observed at country zone

282  stations with average rainfall of 115 mm, equal to 15% of the year) did not favor slurry

283  spreading. Hence, a massive field application of slurry occurred at the beginning of 2020, which

284  led to the consequent observation of high $NH_3$ concentrations. Moreover, during the months

285  of lockdown, transport and industrial activities mostly stopped, and consequently also the

286  related emissions decreased. The reduction of other air pollutants, such as sulfuric acid and

287 nitric acid, with which NH$_3$ combines to form secondary PM (Ge et al., 2020), may have

288 contributed to binding less NH$_3$ and a higher chance to find it in its free form.

289 The main zone differences mentioned above are reported in **Figure 4**. Here, NH$_3$ air

290 concentrations are reported split into 2 periods and 3 zones. In 2020, NH$_3$ concentration

291 recorded at country stations were 69% of the total and were 31% higher than in 2013-2019.

292 No significant differences between NH$_3$ values in 2013-2019 and 2020 can be observed for the

293 city zone (+2%). In the mountain zone, instead, NH$_3$ concentration participates for 10% of the

294 total, with +6% in 2020 compared to 2013-2019. The three zones of city, country, and

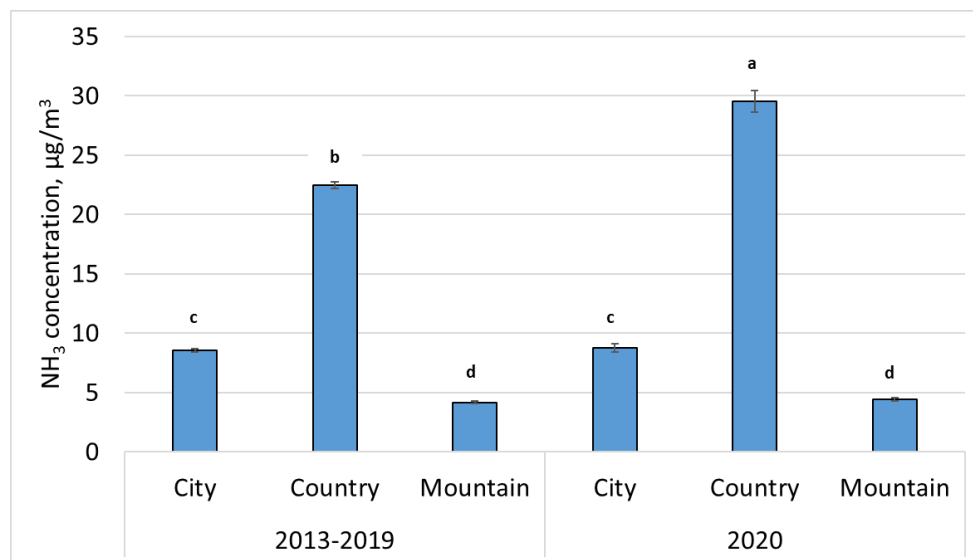295 mountain show statistically significant differences.

296



298 **Figure 4.** Mean and standard error of NH$_3$ concentration, expressed in µg/m$^3$, per zone and

299 period.

300

301 ***3.1.1 Meteorological observations in relation to NH$_3$ air concentration***

302 **Figure 5** reports the average meteorological data of the analyzed provinces, with control units

303 grouped by zone in the two selected periods for temperature (Figure 5-top), rainfall (Figure 5-

304 middle), and wind speed (Figure 5-bottom). Considering that Po Valley is located in Northern

305 Italy and that it is mostly characterized by a temperate climate, without a dry season and with

306 a hot summer (Beck et al., 2018), the meteorological data show a pattern consistent with these

307 characteristics. In particular, regarding temperature a cold winter and a warm summer can be

308 identified; rainfall is concentrated in spring and autumn and wind speed is low on average

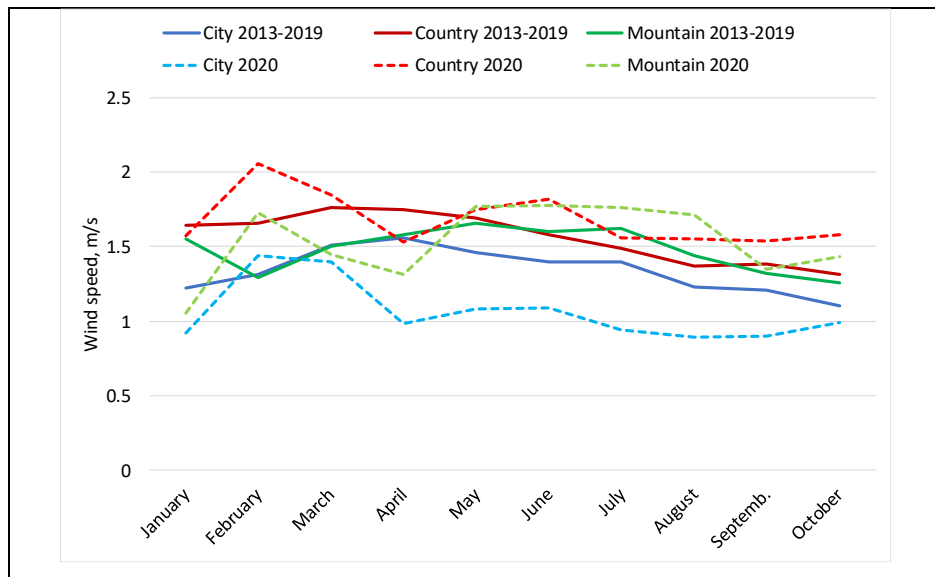309 throughout the year.

310

311
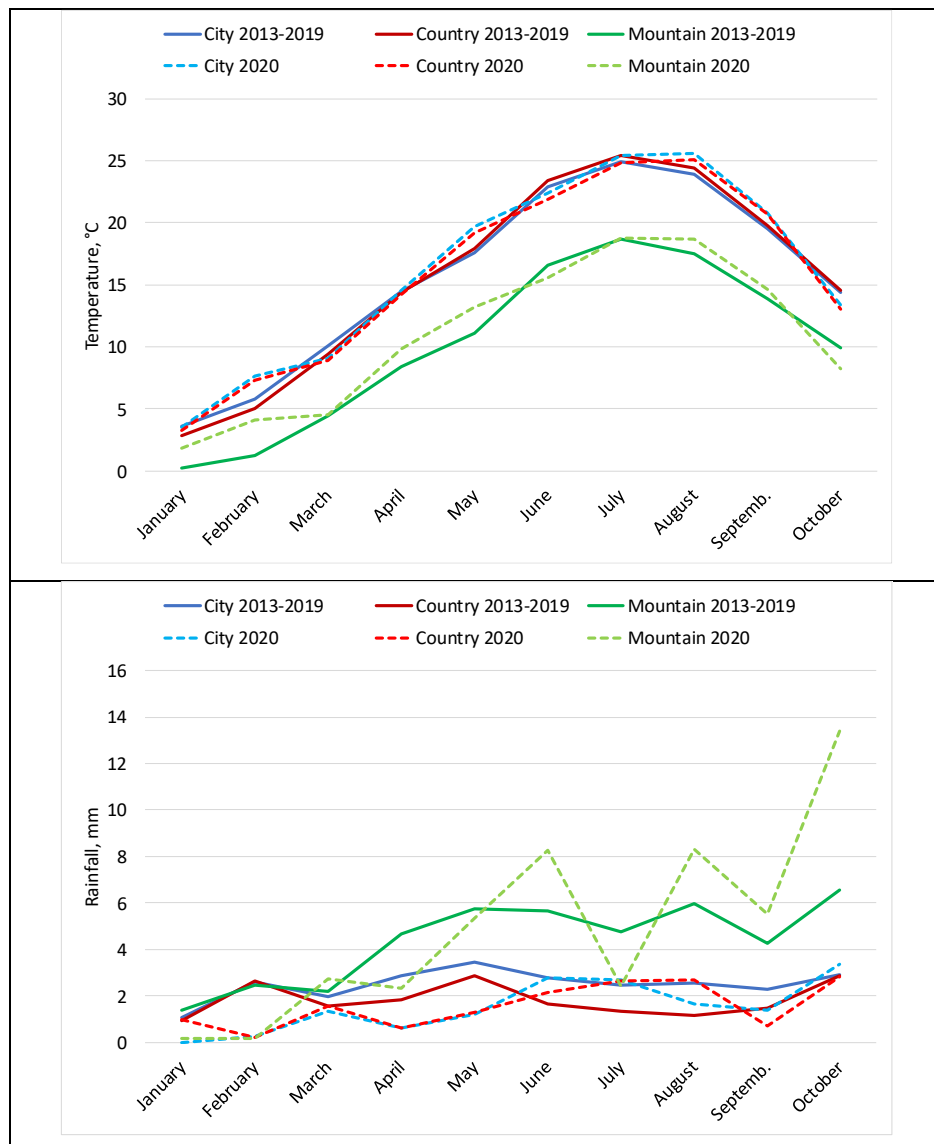
312 **Figure 5.** Mean meteorological data (temperature -top, rainfall – middle, and wind speed -

313 bottom) per zone (city, country, and mountain), month (Jan-Oct) and period (2013-2019,

314 2020).

315

316 In general, it can be observed that both city and country station units recorded similar average

317 yearly values for temperature, with 2020 showing slightly higher values (15.7 and 16.2 °C in

318 2013-2019 and 2020 in the city zone and 15.7 and 15.8°C in the country zone, respectively). In

319 the mountain zone they were lower (10.2 and 10.9°C in 2013-2019 and 2020, respectively).

320 The average rainfall was lower in 2020 compared to the previous period in the city (2.5 and 1.9

321 mm/d in 2013-2019 and 2020, respectively) and country (1.8 and 1.6 mm/d) zones, while in

322 the mountain zone rainfall was higher (4.4 and 4.9 mm/d). As regards wind speed, all values

323 were low: 1.3 and 1.1 m/s as average of 2013-2019 and 2020 in the city zone, country

324 averaging 1.6 and 1.7 m/s and mountain averaging 1.5 m/s in both periods. Pearson

325 correlations were calculated (data not shown) and significant differences were found among

326 all the meteorological parameters considering the different zones and months. Although the

327 linear relationship is not very strong, temperature is significantly negatively correlated with

328    rainfall and wind speed. In contrast, rainfall and wind speed are positively correlated with each

329    other. The changes in NH$_3$ air concentration and meteorological parameters during the period

330    of observation are reported in **Table 2**.

331

| Month | Zone | NH$_3$ | T | R | W |
|---|---|---|---|---|---|
| January | City | -15.4% | -3.3% | -34.0% | -24.6% |
| | Country | 39.6% | 15.5% | 1.0% | -4.3% |
| | Mountain | 6.5% | 682.6% | -87.7% | -32.3% |
| February | City | 62.4% | 32.6% | -90.0% | 9.9% |
| | Country | 105.6% | 44.4% | -91.3% | 24.1% |
| | Mountain | 32.8% | 231.2% | -92.7% | 34.1% |
| March | City | 2.8% | -10.3% | -31.0% | -7.3% |
| | Country | 9.5% | -5.7% | 1.3% | 5.1% |
| | Mountain | 33.2% | 1.6% | 26.0% | -3.3% |
| April | City | 1.1% | 0.5% | -78.7% | -37.2% |
| | Country | 76.7% | -1.0% | -64.9% | -12.6% |
| | Mountain | 41.5% | 16.1% | -50.2% | -17.1% |
| May | City | 48.2% | 11.9% | -64.9% | -26.0% |
| | Country | 48.2% | 6.9% | -54.3% | 3.6% |
| | Mountain | 83.8% | 19.1% | -7.3% | 6.6% |
| June | City | -19.7% | -2.3% | 1.1% | -22.1% |
| | Country | -0.6% | -6.6% | 28.1% | 15.2% |
| | Mountain | -9.8% | -6.1% | 47.0% | 11.3% |
| July | City | -17.5% | 2.2% | 9.7% | -32.9% |
| | Country | 51.4% | -2.2% | 94.8% | 4.7% |
| | Mountain | -1.9% | 0.8% | -49.2% | 8.6% |
| August | City | -5.2% | 7.1% | -34.6% | -27.6% |
| | Country | 14.7% | 2.5% | 133.9% | 13.1% |
| | Mountain | 11.9% | 6.8% | 39.0% | 18.8% |
| September | City | -22.3% | 6.3% | -40.7% | -25.6% |
| | Country | 31.0% | 4.5% | -52.7% | 11.6% |
| | Mountain | -33.7% | 5.5% | 28.7% | 2.3% |
| October | City | 24.2% | -7.3% | 15.3% | -10.0% |
| | Country | -17.6% | -10.3% | -1.4% | 20.6% |
| | Mountain | -49.7% | -16.8% | 104.1% | 13.5% |

332

333    **Table 2.** Percentage change between 2020 and 2013-2019 for $NH_3$ air concentration,

334    temperature (T), rainfall (R) and wind speed (W). When the resulting changes are positive (year

335    2020 > years 2013-2019) cells have a green background.

336

337

338    The relative difference between the periods 2020 and 2013-2019 is carried out by using the

339    data reported in Figure 3 and Figure 5. From these data, it emerges that $NH_3$ concentration in

340    air was higher in 2020 than in the previous period from February to May for all zones and this

341    occurred, in most cases, together with higher temperatures. Except for these four months and

342    October, in city zones $NH_3$ was lower in 2020 than over the previous years, which occurred

343    with changes in the meteorological parameters that, however, do not allow to identify clear

344    links between $NH_3$ and weather patterns, and especially with rainfall/wind speed.

345    To clarify the relationships among these variables, a GLM procedure was performed to obtain

346    a predictive model for $NH_3$ concentration in air. The model was generated on the classes of

347    year (2 levels: 2013-2019 and 2020) and zone (3 levels: city, country, and mountain) and was

348    found statistically significant, although with a very low coefficient of determination ($R^2$=0.19).

349    All variables were also significant with "year" and "zone" very significant (p<0.0001) and

350    month, weather parameters and their interactions significant (p<0.05). Among the

351    meteorological parameters, rainfall was the variable with the lowest significance for the

352    prediction of $NH_3$. The calculated Least Squares Means (LS Means) were all significant

353    (p<0.0001). However, the statistical significance of LS Means for the effect year*zone showed

354    no difference between the 2 periods for the city and the mountain zones as reported in **Table**

355    **3**.

356

357

| i/j | 2013-2019 country | 2013-2019 mountain | 2020 city | 2020 country | 2020 mountain |
|---|---|---|---|---|---|
| 2013-2019 city | *** | *** | n.s. | *** | *** |
| 2013-2019 country | | *** | *** | *** | *** |
| 2013-2019 mountain | | | *** | *** | n.s. |
| 2020 city | | | | *** | *** |
| 2020 country | | | | | *** |

Notes: ***=p<0.0001; n.s.=not significant

Table 3. Statistical significance of Least Squares Means resulting from the GLM procedure for the effect year*zone and $NH_3$ as dependent variable.

361

This result shows that, in the two studied periods, both city zones and mountain zones have comparable results. Since $NH_3$ is mostly released in countryside areas and normally deposited within a short radius from the emissive source, it can be expected that lower concentrations reach cities and mountain zones and that these latter do not show significant differences in the analyzed periods. Since agricultural activities are more subject than others to annual variability and seasonality, the fact that $NH_3$ in countryside areas is significantly different between 2013-2019 and 2020 prompted us to investigate the effects of seasonality on $NH_3$ every year. Thus, the model was relaunched evaluating the effect of each year on $NH_3$, focusing only on the country zone. This model was found significant with the coefficient of determination $R^2=0.29$ and all weather parameters significant (p<0.05). Significant differences for $NH_3$ concentration emerged in some years, while no differences were found between (i) 2013 and 2016, (ii) 2014 and 2015, and (iii) 2017, 2018 and 2020. The results of this second

374 analysis suggest that meteorological variability can play a role on $NH_3$ air concentration in

375 country zones.

376
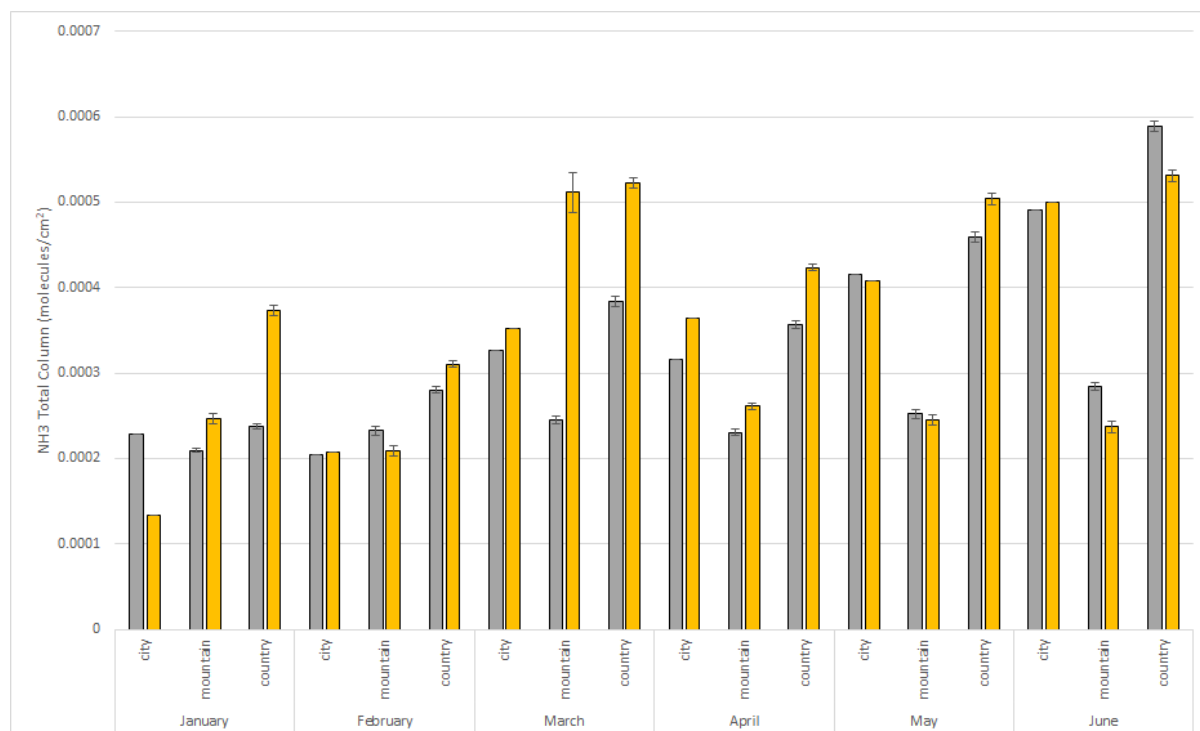
377 **3.2 Satellite measurements**



378
379 **Figure 6**. Mean and standard error of total column $NH_3$ from IASI observations for each month

380 (January-June) over the period 2013-2019 and 2020 for each of the three zones considered

381 (city, mountain, country).

382

383 The $NH_3$ total column observations from IASI data reported in **Figure 6** show slightly different

384 patterns compared to ground measurements, although it is a shared feature that country

385 zones show the highest values in all months during 2013-2019 and in 2020. The highest total

386 column $NH_3$ was recorded for grid points classified as "country" in June, both over 2013-2019

387 ($5.89e^{-4}$ mol/cm$^2$) and in 2020 ($5.31e^{-4}$ mol/cm$^2$); over 2013-2019, May was the second highest

388 month with respect to $NH_3$ values ($4.59e^{-4}$ mol/cm$^2$), while in 2020 it was March, when the

389    lockdown started ($5.22e^{-4}$ mol/cm$^2$). In March 2020, mountain grid points also show very high

390    values ($5.11e^{-4}$ mol/cm$^2$), possibly because of the actual inclusion of agricultural areas within

391    grid points classified as mountain at the IASI scale (maximum agricultural cover was 21% in

392    mountain grid points from CLC 2018). As a further hint of this, compared to ground

393    observations, city zones show generally lower total column $NH_3$ than mountain zones, with the

394    lowest values overall recorded for city zones in January 2020 ($1.34e^{-4}$ mol/cm$^2$). For country

395    zones, all months except June show an increase in total column $NH_3$ compared to the average

396    of 2013-2019. For the other zones, the pattern is more variable: city grid points show a higher

397    $NH_3$ total column in February, March, April, and June 2020 while for mountain stations the

398    months with a higher $NH_3$ total column are January, March (with an increase of 108%

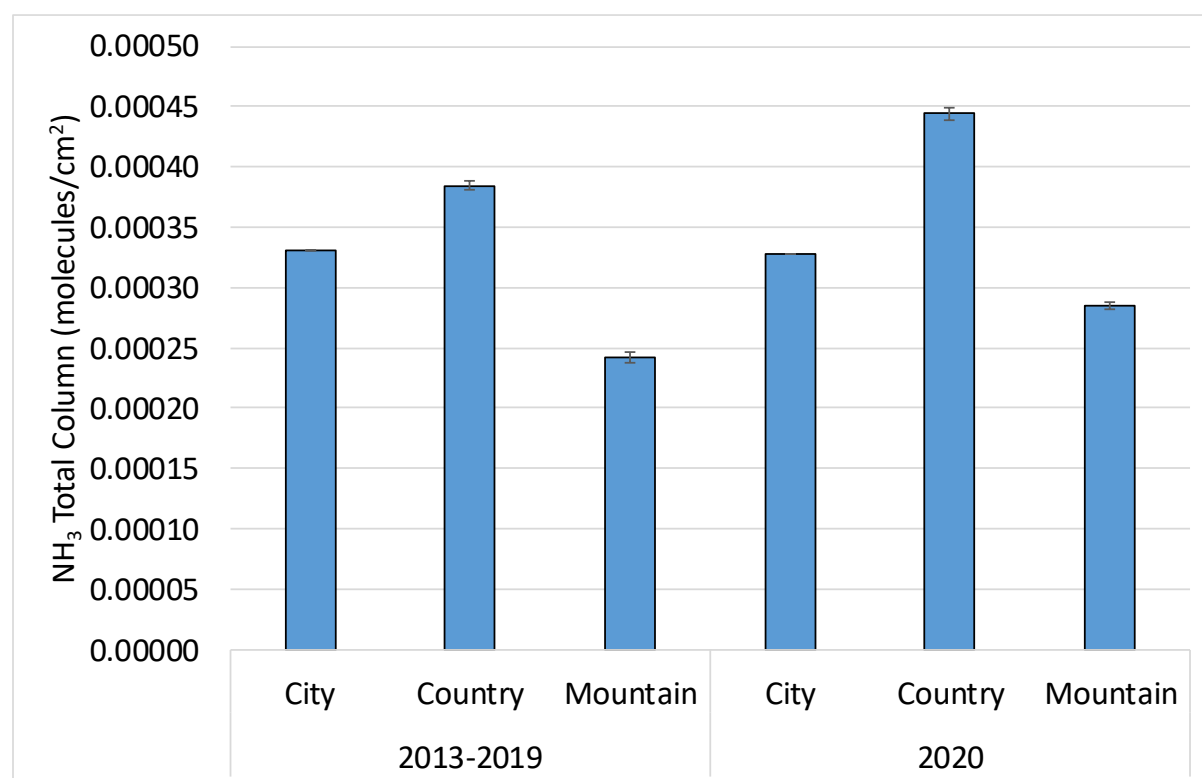399    compared to the same month over 2013-2019), April and June.

400

401

402

403    **Figure 7**. Mean and standard error of $NH_3$ total column for January-June in 2013-2019 and 2020

404    for the three zones considered (city, mountain, country).

405

406    As shown in **Figure 7**, averaging all monthly observations between January and June, mountain

407    and country zones show an increase in $NH_3$ total column in 2020 compared to 2013-2019, with

408    similar values (18% for mountain zones and 15% for country zones).

409    As for ground observations, the $NH_3$ total column for city zones is unvaried between the two

410    periods (-0.73%). In contrast with ground observations, however, the share of $NH_3$ for the

411    different zones is more uniform: in 2020, country zones accounted for 42% of the total column,

412    mountain zones for 27% and city zones for 31%. This might be caused by the coarse spatial grid

413    of IASI measurements and mix between different land use classes at the IASI scale

414

415    ***3.2.1 Meteorological observations in relation to NH₃ air concentration***

416    As for ground observations, monthly meteorological data and $NH_3$ total column divided in the

417    two periods were compared. **Table 4** reports such results.

418

| Month | Zone | $NH_3$ | T | R | W |
|-------|------|--------|---|---|---|
| January | City | -41.30% | 12.53% | -81.74% | -15.22% |
| | Country | 57.09% | 8.67% | -66.28% | -5.94% |
| | Mountain | 17.62% | 50.67% | -69.93% | -2.42% |
| February | City | 1.53% | 50.45% | -87.94% | -1.07% |
| | Country | 10.67% | 48.31% | -90.94% | 48.47% |
| | Mountain | -9.82% | 449.99% | -66.97% | 32.27% |
| March | City | 7.72% | -5.11% | -4.30% | 4.73% |
| | Country | 36.02% | -4.51% | -22.97% | 46.01% |
| | Mountain | 108.41% | -5.71% | 14.73% | -9.26% |
| April | City | 15.62% | 3.15% | -57.28% | -47.02% |
| | Country | 18.64% | -0.05% | -52.21% | -24.42% |

| | | | | | |
|---|---|---|---|---|---|
| | Mountain | 13.32% | 9.78% | -57.93% | 28.69% |
| May | City | -1.68% | 9.32% | -10.92% | 24.81% |
| | Country | 9.80% | 9.55% | -36.25% | 46.39% |
| | Mountain | -2.54% | 16.17% | -12.84% | 26.45% |
| June | City | 1.84% | -7.49% | 49.63% | -11.88% |
| | Country | -9.85% | -5.65% | 47.79% | 41.90% |
| | Mountain | -16.59% | 9.58% | 44.44% | 32.56% |

**Table 4.** Percentage change between 2020 and 2013-2019 for $NH_3$ total column, temperature (T), rainfall (R) and wind speed (W) from IASI and ERA-5 observations. When the resulting changes are positive (year 2020 > years 2013-2019) cells have a green background.

In most months, temperature was higher in 2020 than in 2013-2019, particularly in the mountain zones where it was always higher except for March, with an increase of 449.99% in February 2020 compared to 2013-2019. In contrast, precipitation was lower in most months, except for mountain zones in March and all zones in June, while wind speed showed a more varied pattern with a decrease in January 2020 and an increase in May 2020 in all zones.

A GLM procedure was carried out to identify a prediction model for $NH_3$ total column, in a similar way as done for ground-based measurements. The model was found significant with a coefficient of determination of 0.55. The main difference with the GLM for ground-based observations is related to the fact that none of the meteorological parameters was found statistically significant, and only the zone parameter and month*zone effect were significant in the prediction of $NH_3$. In addition, no statistical difference emerged from the evaluation of LS Means for year*zone, as reported in **Table 5**.

| i/j | 2013-2019 country | 2013-2019 mountain | 2020 city | 2020 country | 2020 mountain |
|---|---|---|---|---|---|

| | | | | | |
|---|---|---|---|---|---|
| 2013-2019 city | n.s. | n.s. | n.s. | n.s. | n.s. |
| 2013-2019 country | | n.s. | n.s. | n.s. | n.s. |
| 2013-2019 mountain | | | n.s. | n.s. | n.s. |
| 2020 city | | | | n.s. | n.s. |
| 2020 country | | | | | n.s. |

437    **Table 5.** Statistical significance of LS Means resulting from the GLM procedure for the effect

438    year*zone and $NH_3$ as dependent variable.

439

440    The result of the GLM procedure with satellite $NH_3$ observations and meteorological

441    parameters shows no statistical difference with respect to the $NH_3$ concentration in the air

442    between the two periods. This is in contrast with the ground-based measurements, which

443    showed a significant difference for $NH_3$ concentrations in country stations, between 2013-

444    2019 and 2020. The reason for this result may be due to the susceptibility of control units to a

445    series of site-specific aspects that, instead, cannot be measured in the satellite coarse grid, and

446    the fact that satellites measure total column $NH_3$, which might be the result of emissions

447    originating in a different grid point than the footprint observed by the satellite at the time of

448    data acquisition.

449

450    **4. Discussion**

451    This study was carried out with a focus on comparing the period (i.e., from year 2013 to 2019)

452    before the lockdown determined by the emergency of COVID-19 and the subsequent period

453    during the pandemic (i.e., year 2020, with the strict lockdown lasting from March-June 2020),

454    adopting two measurement systems. Remote sensing datasets show no significant difference

455    in $NH_3$ air concentration between the period before the spread of COVID-19 and the one during

456    the pandemic. From the ground based analysis, $NH_3$ was observed higher than other years in

457 city and mountain, and significantly in country zones. As $NH_3$ is strongly dependent on

458 agricultural and livestock activities, its concentration was found subject to seasonality, weather

459 conditions and to agricultural management. This aspect has been underlined also in the study

460 of Lonati and Cernuschi (2020) and Deserti et al. (2020). The same result was observed also by

461 Gualtieri et al. (2020) who state that, in 2020, $NH_3$ concentration increased in Italy compared

462 to 2019. They also report that more than 90% of $NH_3$ is of agricultural origin in Milan, while

463 this contribution decreases to 71% in Rome and 62% in Bologna, suggesting once more the

464 relevance of livestock activities in Northern Italy. Therefore, the role of agriculture and

465 livestock appears to be the largest influence on $NH_3$ air concentrations. Given the relationship

466 of weather and seasonality with agricultural field activities, and the characteristics of

467 $NH_3$ emissions (Brentrup et al., 2000; Sutton et al., 2013), it can be expected that $NH_3$

468 concentration is higher in summer (high temperatures) than in winter (when regulations

469 prohibit field spreading due to nitrate leaching), and that peaks are observed in periods before

470 crop cultivation (generally from February to June and from August to October in the analyzed

471 area, where double cropping is widespread) when base-dressing fertilizers are applied on the

472 field (Guido et al., 2020; Pedersen et al., 2020). All these aspects are confirmed also by the

473 present study. Independently from the period considered, the highest $NH_3$ concentration can

474 be observed in February-March and July-October, compared to the other months.

475 Moreover, different values in $NH_3$ concentration are strictly linked to manure storage (Zilio et

476 al., 2020) and to field application, since this operation can be carried out when no rainfall

477 occurs and in agreement with the European nitrates directive 91/676/EEC and the regional

478 action programs for the protection of water pollution caused by nitrates from agricultural

479 sources. These aspects have been widely investigated in literature, such as by Skjøth et al.

480 (2011), Ramanantenasoa et al. (2018), and Ge et al. (2020).

481

482

### 4.1 Limitations of ground-based and satellite observations

484
485    In this study, measurements from both ground control units and satellite sensors were used to

486    investigate air concentrations of $NH_3$. The two techniques showed similar patterns, such as the

487    higher yearly average concentrations in country zones in 2020 compared to 2013-2019 but

488    also some differences for individual months and in the relative contribution of the different

489    zones to total $NH_3$ concentrations, which are related to the limitations inherent in

490    measurement techniques.

491    For the entire Lombardy region (surface area about 23000 $km^2$), the availability of $NH_3$

492    measured data for the analyzed period was limited to 10 control units for the assessment using

493    ground stations. However, $NH_3$ concentration may vary considerably within few kilometers

494    (Lonati and Cernuschi, 2020). This confirms the scarcity of $NH_3$ control units compared to other

495    air pollutants; in fact, in the same area available stations amount to 90 units for $PM_{10}$ and 38

496    units for $PM_{2.5}$ (ARPA Lombardia, 2020). Moreover, for the same control units, air

497    concentrations of different pollutants, such as $NH_3$ and PM, are not always available, making

498    comparisons more difficult.

499    As concerns satellite images, the number of measurements, after filtering for observations

500    with high uncertainty, did not allow us to create a grid finer than 0.5x0.5°, which would have

501    introduced a large number of data gaps. The coarse grid however complicates the assessment

502    of local variability; the comparison between data gathered from each ground based control

503    unit and satellite observations is problematic because of 1) the different spatial resolution; in

504    fact, ground stations classified as "city" might be included in country zones in IASI pixels, with

505      a much larger contribution of $NH_3$ air concentration from agricultural areas; 2) the different

506      unit of measure and assessment method, as one is a ground level observation, the other is a

507      column observation. An attempt to correlate monthly data from ground and satellite

508      observations showed an $r^2$ of 0.21-0.29; this is in line with Van Damme et al. (2015), who report

509      Pearson's correlations of 0.28 comparing monthly data from IASI and ground observations

510      from a global network, ranging from 0.81 (Russian Fyodorovskoye site, with very high $NH_3$

511      concentrations owing to fire events) to negative correlations at several sites in Finland,

512      probably caused by the low concentrations at these sites in association with low temperatures

513      and thus the low thermal contrast of IASI.

514      Given the limitations of both measurement approaches, among which the temporal and spatial

515      resolution, improvements should be introduced both in the number and density of ground

516      stations, especially in areas where agriculture is widespread, and in the availability of satellite

517      data with a higher spatial resolution, which might also make validation efforts easier in

518      comparison with ground observations.

519

520      ## 4.2 Prospects for improving air quality and opportunities for further study

521

522      In the future, a significant reduction in $NH_3$ air concentrations is expected as a consequence of

523      the abatement measures that are being introduced in agricultural and livestock farms (e.g.,

524      closed tank storages, manure and slurry treatments, precision application of slurry on field)

525      (Finzi et al., 2019; Zilio et al., 2020), although these measures are currently present only in few

526      contexts. Considerable improvements have already been introduced in the European Union,

527      which brought to a strong reduction of $NH_3$ air concentration, reaching -24% from 1990 to

528    2017 (Costantini et al., 2020). However, this trend of reduction is proceeding further; in fact,

529    in some countries, regions, and farms additional improvements are being introduced or are

530    under study. For example, Miranda et al. (2021) investigated through the Life Cycle Assessment

531    method, the environmental implications of treating slurry and found positive results for the

532    reduction of gases, among which $NH_3$, with the addition of sulfuric acid to slurry. Slurry

533    acidification was found effective in reducing $NH_3$ and other greenhouse gases (GHGs) also by

534    Fangueiro et al. (2015). However, supporting farmers in the direction of abating $NH_3$ is

535    fundamental to increase the spread of such ameliorative techniques and solutions. The chief

536    aspects on which to focus include efficient livestock rearing techniques supported by

537    technology, balanced animal feed rations, air scrubbers in barns, adequate manure

538    management with frequent removal from the barn, manure treatments such as anaerobic

539    digestion, solid-liquid separation, slurry acidification, proper manure storage with closed tanks

540    and proper field application with precision application equipment (Guido et al., 2020; Regueiro

541    et al., 2016).

542    Importantly from the environmental point of view, avoiding $NH_3$ losses can lead to maintaining

543    nutrients in the manure/slurry and therefore applying more nutrients to the soil when

544    spreading manure or slurry, thus requiring fewer mineral fertilizers and bringing benefits to

545    the environmental sustainability, plus valorizing an already available resource that is free of

546    charge. Finally, while high $NH_3$ concentration in air may represent a local issue, damages to

547    ecosystems from $NH_3$ are not only local and are widely investigated due to the main effects of

548    acidification and eutrophication on biodiversity loss in coastal and estuarial areas, such as in

549    the study by Vetterli et al. (2016).

550     Despite the improvements in agricultural practices, this study has shown that $NH_3$

551     concentrations in air remained high in areas such as the Po Valley even during the lockdown

552     caused by the spread of COVID-19. To further validate the considerations made regarding $NH_3$

553     air concentrations during 2020, future research should consider a wider area (e.g. Italy,

554     Europe), as well as expand the analysis to other air pollutants. To this end, it would also be

555     interesting to integrate ground-based and satellite datasets with physico-chemical dispersion

556     models (e.g. LOTOS-EUROS, Schaap et al., 2008; also employed by Van Damme et al. 2014;

557     2015) to better understand their origin and interactions, while in this study a purely statistical

558     comparative approach was adopted.

559

560

561     **5. Conclusions**

562     This study aimed to evaluate the atmospheric concentrations of $NH_3$ during the spread of the

563     COVID-19 pandemic in Northern Italy and the related changes in anthropogenic activities. For

564     this purpose, ground-based and satellite measurement data relating to 2020 were analyzed

565     and compared with previous years (2013-2019). Ground-based measurements showed

566     statistically significant differences between the two periods in the country areas, where $NH_3$

567     was found higher in 2020 (+31% compared to the 2013-2019 average); on the other hand, no

568     significant differences emerged for the city and mountain areas. Satellite data show similar

569     patterns, but no significant differences between the two periods and less spatial variability

570     between city, country, and mountain areas, probably due to the coarse spatial grid of IASI

571     measurements. Contrary to other air pollutants, it can be concluded that no $NH_3$ reduction

572     effect has occurred as a consequence of the anti-COVID-19 measures, which can be explained

573 by the non-interruption of agricultural activities, the main emissive source of this pollutant.

574 The integration between datasets from different measurement sources allows having a

575 broader understanding of atmospheric phenomena, since both methods alone have their

576 limitations. These considerations offer insights into the physico-chemical modeling of this

577 pollutant and the actions aimed at its mitigation.

578

579 **References**

580 Altuwayjiri A., Soleimanian E., Moroni S., et al., 2021. The impact of stay-home policies during

581 Coronavirus-19 pandemic on the chemical and toxicological characteristics of ambient PM2.5 in the

582 metropolitan area of Milan, Italy. Science of the Total Environment, 758 (1), 143582.

583 https://doi.org/10.1016/j.scitotenv.2020.143582

584 Arpa Lombardia, 2020. Agenzia Regionale per la Protezione dell'Ambiente – Lombardia.

585 https://www.arpalombardia.it/Pages/ARPA_Home_Page.aspx, Last accessed 9 November 2020.

586 Beck, H., Zimmermann, N., McVicar, T., Vergopolan, N., Berg, A., Wood, E.F., 2018. Present and

587 future Köppen-Geiger climate classification maps at 1-km resolution. Scientific Data, 5, 180214.

588 https://doi.org/10.1038/sdata.2018.214

589 Bonati, M., Campi, R., Zanetti, M., Cartabia, M., Scarpellini, F., Clavenna, A., Segre, G., 2021.

590 Psychological distress among Italians during the 2019 coronavirus disease (COVID-19) quarantine. BMC

591 Psychiatry, 21, 20. https://doi.org/10.1186/s12888-020-03027-8

592 Brentrup, F., Küsters, J., Lammel, J., Kuhlmann, H., 2000. Methods to estimate on-field nitrogen

593 emissions from crop production as an input to LCA studies in the agricultural sector. International

594 Journal of Life Cycle Assessment. 5, 349-357. https://doi.org/10.1007/BF02978670

595 Buganza, E., Donzelli, M., Gurrieri, G.L., Lazzarini, M., Scotto Di Marco, E., Bravetti, E., Dal Santo,

596 U., Di Leo, A., Lanzani, G., Cazzuli, O., Minardi, G.P., 2020. Preliminary analysis of air quality in Lombardy

597    during the COVID-19 emergency (in Italian). Agenzia Regionale per la Protezione dell'Ambiente –

598    Lombardia.                              Available                              at

599    https://www.arpalombardia.it/sites/DocumentCenter/Documents/Aria%20-

600    %20Relazioni%20approfondimento/Analisi%20preliminare%20QA-COVID19.pdf,    Last

601    accessed 9 November 2020.

602    Collivignarelli M.C., Abbà A., Bertanza G., Pedrazzani R., Ricciardi P., Miino M.C., 2020.

603    Lockdown for CoViD-2019 in Milan: What are the effects on air quality? Science of The Total

604    Environment, 732, 139280. https://doi.org/10.1016/j.scitotenv.2020.139280

605    Costantini, M., Bacenetti, J., Coppola, G., Orsi, L., Ganzaroli, A., Guarino, M., 2020.

606    Improvement of human health and environmental costs in the European Union by air

607    scrubbers in intensive pig farming. Journal of Cleaner Production, 275, 1244007.

608    https://doi.org/10.1016/j.jclepro.2020.124007

609    Deserti et al., 2020. Report 2 COVID-19. Preliminary study of the effects of COVID-19 measures

610    on emissions in the atmosphere and on quality of the air in the Po Valley (in Italian). Report from the

611    LIFE    PrepAIR    project,    August    2020.    Available    at    https://www.lifeprepair.eu/wp-

612    content/uploads/2020/09/COVIDQA-Prepair-2-17Settembre2020.pdf,    Last    accessed    14

613    December 2020.

614    DPCM, 2020. Decree of the President of the Council of Ministers of the Italian Republic of

615    March 22, 2020 - Further Implementing Provisions of the Decree-Law of February 23, 2020, n. 6,

616    Containing Urgent Measures Regarding the Containment and Management of the Epidemiological

617    Emergency from COVID-19 (in Italian). President of the Council of Ministers of the Italian Republic,

618    Rome, Italy. Available at https://www.gazzettaufficiale.it/eli/id/2020/03/22/20A01807/sg, Last

619    accessed 14 December 2020.

620     EEA (European Environmental Agency), 2019. European Union Emission Inventory Report

621     1990-2017, under the UNECE Convention on Long-Range Transboundary Air Pollution (CLRTAP). EEA

622     Report | No 08/2019.

623     EMEP Centre on Emission Inventories and Projections, 2020. Available at

624     https://www.ceip.at/webdab-emission-database. Last accessed 02 February 2021.

625     European Commission, 2005. Communication from the commission to the council and

626     the European Parliament. "Thematic Strategy on air pollution". Available at

627     https://ec.europa.eu/environment/archives/cafe/pdf/annex_sec_2005_1132_en.pdf.     Last

628     accessed 02 February 2021.

629     Erisman, J., Bleeker, A., Galloway, J., Sutton, M., 2007. Reduced nitrogen in ecology and the

630     environment.     Environmental     Pollution,     150,     140–149.     https://doi.org/10.1016/j.envpol.

631     2007.06.033.

632     Executive Body of the Convention on Long-Range Transboundary Air Pollution, 2019. Draft of

633     Assessment     Report     on     Ammonia.     Available     at

634     https://unece.org/fileadmin/DAM/env/documents/2019/AIR/EMEP_WGE_Joint_Session/As

635     sessment_Report_on_Ammonia_20190827.pdf. Last Accessed 02 February 2021.

636     Fangueiro, D., Pereira, J., Bichana, A., Surgy, S., Cabral, F., Coutinho, J., 2015. Effects of cattle-

637     slurry treatment by acidification and separation on nitrogen dynamics and global warming potential

638     after surface application to an acidic soil. Journal of Environmental Management, 162, 1-8.

639     https://doi.org/10.1016/j.jenvman.2015.07.032

640     Feranec, I., Soukup, T., Hazeu, G., Jaffrain, G. (Eds.), 2016. European Landscape Dynamics. CRC

641     Press, Boca Raton.

642     Finzi, A., Riva, E., Bicoku, A., Guido, V., Shallari, S., Provolo, G., 2019. Comparison of techniques

643     for ammonia emission mitigation during storage of livestock manure and assessment of their effect in

644   the    management    chain.    Journal    of    Agricultural    Engineering,    50,    12–19.

645   https://doi.org/10.4081/jae.2019.881

646   Ge, X., Schaap, M., Kranenburg, R., Segers, A., Reinds, G. J., Kros, H., de Vries, W., 2020.

647   Modeling atmospheric ammonia using agricultural emissions with improved spatial variability and

648   temporal    dynamics,    Atmospheric    Chemistry    and    Physics,    20,    16055–16087,

649   https://doi.org/10.5194/acp-20-16055-2020.

650   Gualtieri, G., Brilli, L., Carotenuto, F., Vagnoli, C., Zaldei, A., Gioli, B., 2020. Quantifying road

651   traffic impact on air quality in urban areas: A Covid19-induced lockdown analysis in Italy. Environmental

652   Pollution, 267, 115682.

653   Guido, V., Finzi, A., Ferrari, O., Riva, E., Quílez, D., Herrero, E., Provolo, G., 2020. Fertigation of

654   maize with digestate using drip irrigation and pivot systems. Agronomy, 10, 10, 1453. Doi:

655   10.3390/agronomy10101453

656   ISMEA,    2019a.    Settore    lattiero    caseario    -    Scheda    di    settore.

657   http://www.ismeamercati.it/flex/cm/pages/ServeBLOB.php/L/IT/IDPagina/3521.   (Last   accessed   14

658   December 2020).

659   ISMEA,    2019b.    Allevamento    bovino    da    carne    –    Scheda    di    settore.

660   http://www.ismeamercati.it/flex/cm/pages/ServeBLOB.php/L/IT/IDPagina/3515.   (Last   accessed   14

661   December 2020).

662   ISMEA,    2019c.    Settore    suinicolo    –    Scheda    di    settore.

663   http://www.ismeamercati.it/flex/cm/pages/ServeBLOB.php/L/IT/IDPagina/3516.   (Last   accessed   14

664   December 2020).

665   ISMEA, 2020. Filiera avicola – Scheda di settore. http://www.ismeamercati.it/carni/avicoli-uova

666   (Last accessed 14 December 2020)

667    Li, T., Hu, R., Chen, Z., Li, Q., Huang, S., Zhu, Z., Zhou, L.-F., 2018. Fine particulate matter

668    (PM2.5): the culprit for chronic lung diseases in China. Chronic Diseases and Translational

669    Medicine 4, 176–186.

670    Lonati G., Cernuschi, S., 2020. Temporal and spatial variability of atmospheric

671    ammonia in the Lombardy region (Northern Italy). Atmospheric Pollution Research 11, 2154–

672    2163. https://doi.org/10.1016/j.apr.2020.06.004

673    Lovarelli, D., Conti, C., Finzi, A., Bacenetti, J., Guarino, M., 2020. Describing the trend of

674    ammonia, particulate matter and nitrogen oxides: the role of livestock activities in northern Italy during

675    Covid-19       quarantine.       Environmental       Research,       191,       110048.

676    https://doi.org/10.1016/j.envres.2020.110048

677    Manigrasso, M., Protano, C., Guerriero, E., Vitali, M., Avino, P., 2020. May SARS-CoV-

678    2 diffusion be favoured by alkaline aerosols and ammonia emissions? Atmosphere, 11, 995.

679    doi:10.3390/atmos11090995

680    Miranda, C., Soares, A.S., Coelho, A.C., Trinidade, H., Teixeira, C.A., 2021.

681    Environmental implications of stored cattle slurry treatment with sulphuric acid and biochar:

682    A    life    cycle    assessment    approach.    Environmental    Research,    194,    110640.

683    https://doi.org/10.1016/j.envres.2020.110640

684    Nair, A.A.; Yu, F, 2020. Quantification of Atmospheric Ammonia Concentrations: A Review of Its

685    Measurement and Modeling. Atmosphere, 11, 1092. https://doi.org/10.3390/atmos11101092

686    Nitrates Directive (Eu), 2016. 2016/2284 of the European Parliament and of the Council of 14

687    December 2016 on the reduction of national emissions of certain atmospheric pollutants, amending

688    Directive 2003/35/EC and repealing Directive 2001/81/EC. OJ L 344/1, 17.12.

689    Nuñez-Delgado A., Zhou Y., Domingo J.L., 2021. Editorial of the VSI "Environmental, ecological

690    and public health considerations regarding coronaviruses, other viruses, and other microorganism

691    potentially causing pandemic diseases". Environmental Research, 192, 110322.

692    https://doi.org/10.1016/j.envres.2020.110322

693    Pedersen, I.F., Rubaek, G.H., Nyord, T., Sorensen, P., 2020. Row-injected cattle slurry

694    can replace mineral P starter fertiliser and reduce P surpluses without compromising final

695    yields of silage maize. European Journal of Agronomy, 116, 126057.

696    https://doi.org/10.1016/j.eja.2020.126057

697    Perone G., 2021. The determinants of COVID-19 case fatality rate (CFR) in the Italian regions

698    and provinces: An analysis of environmental, demographic, and healthcare factors. Science of the Total

699    Environment, 755 (1), 142523. https://doi.org/10.1016/j.scitotenv.2020.142523

700    Raffaelli, K.; Deserti, M.; Stortini, M.; Amorati, R.; Vasconi, M.; Giovannini, G., 2020. Improving

701    Air Quality in the Po Valley, Italy: Some Results by the LIFE-IP-PREPAIR Project. Atmosphere , 11, 429.

702    https://doi.org/10.3390/atmos11040429

703    Ramanantenasoa, M.M.J., Gilliot, J.M., Mignolet, C., Bedos, C., Mathias, E., Eglin, T., Makowski,

704    D., Genermont, S., 2018. A new framework to estimate spatio-temporal ammonia emissions due to

705    nitrogen fertilization in France. Science of the Total Environment, 645, 205–219.

706    https://doi.org/10.1016/j.scitotenv.2018.06.202

707    Regueiro, I., Coutinho, J., Gioelli, F., Balsari, P., Dinuccio, E., Fangueiro, D., 2016.

708    Acidification of raw and co-digested pig slurries with alum before mechanical separation

709    reduces gaseous emission during storage of solid and liquid fractions. Agriculture, Ecosystems

710    and Environment, 227, 42-51. http://dx.doi.org/10.1016/j.agee.2016.04.016

711    Schaap, M., Timmermans, R., Roemer, M., Boersen, G. Builtjes, P., Sauter, F., Velders, G., Beck,

712    J., 2008. The LOTOS-EUROS model: Description, validation and latest developments, International

713    Journal of Environment and Pollution, 32, 270–290, doi:10.1504/IJEP.2008.017106.

714        Skjøth, C. A., Geels, C., Berge, H., Gyldenkærne, S., Fagerli, H., Ellermann, T., Frohn, L. M.,

715        Christensen, J., Hansen, K. M., Hansen, K., and Hertel, O., 2011. Spatial and temporal variations in

716        ammonia emissions – a freely accessible model code for Europe, Atmospheric Chemistry and Physics,

717        11, 5221–5236, https://doi.org/10.5194/acp-11-5221-2011.

718        Srivastava A., 2021. COVID-19 and air pollution and meteorology – an intricate relationship: A

719        review. Chemosphere. 263, 128297. https://doi.org/10.1016/j.chemosphere.2020.128297

720        Sutton, M. A., Reis, S., Riddick, S. N., Dragosits, U., Nemitz, E., Theobald, M. R., Tang, Y. S.,

721        Braban, C. F., Vieno, M., Dore, A. J., Mitchell, R. F., Wanless, S., Daunt, F., Fowler, D., Blackall, T. D.,

722        Milford, C., Flechard, C. R., Loubet, B., Massad, R., Cellier, P., … de Vries, W., 2013. Towards a climate-

723        dependent paradigm of ammonia emission and deposition. Philosophical transactions of the Royal

724        Society    of    London.    Series    B,    Biological    sciences,    368(1621),    20130166.

725        https://doi.org/10.1098/rstb.2013.0166

726        Van Damme, M., Wichink Kruit, R.J., Schaap, M., Clarisse, L., Clerbaux, C., Coheur, P.-F.,

727        Dammers, E., Dolman, A.J., Erisman, J.W., 2014. Evaluating 4 years of atmospheric ammonia (NH3) over

728        Europe using IASI satellite observations and LOTOS-EUROS model results. Journal of Geophysical

729        Research: Atmospheres, 119, 9549–9566. https://doi.org/10.1002/2014JD021911

730        Van Damme, M., Clarisse, L., Dammers, E., Liu, X., Nowak, J. B., Clerbaux, C., Flechard, C. R.,

731        Galy-Lacaux, C., Xu, W., Neuman, J. A., Tang, Y. S., Sutton, M. A., Erisman, J. W., and Coheur, P. F., 2015.

732        Towards validation of ammonia (NH3) measurements from the IASI satellite, Atmospheric

733        Measurement Techniques, 8, 1575–1591.

734        Vetterli, A., Hietanen, S., Leskinen, E., 2016. Spatial and temporal dynamics of ammonia

735        oxidizers    in    the    sediments.    Marine    Environmental    Research,    113,    153-163.

736        http://dx.doi.org/10.1016/j.marenvres.2015.12.008

737        Zambrano-Monserrate M.A., Ruano M.A., Sanchez-Alcade L., 2020. Indirect effects of COVID-

738        19 on the environment. Science of the Total Environment, 728, 138813.

739        https://doi.org/10.1016/j.scitotenv.2020.138813

740        Zheng, G., Su, H., Wang, S., Andreae, M.O., Pöschl, U., Cheng, Y., 2020. Multiphase

741        buffer theory explains contrasts in atmospheric aerosol acidity. Science, 369, 1374-1377.

742        Zilio, M., Orzi, V., Chiodini, M.E., Riva, C., Acutis, M., Boccasile, G., Adani, F., 2020. Evaluation

743        of ammonia and odour emissions from animal slurry and digestate storage in the Po Valley (Italy). Waste

744        Management. 103, 296–304. https://doi.org/10.1016/j.wasman.2019.12.038

745